

Transport Properties of LiTFSI-Acetamide Room Temperature Molten Salt Electrolytes Applied in an Li-Ion Battery

Chao-Chen Yang^a, Hsin-Yi Hsu^b, and Chen-Ruei Hsu^a

^a Department of Chemical Engineering, National Yunlin University of Science and Technology, 123 University Road, Sec. 3, Yunlin, Taiwan, R.O.C.

^b Department of Environmental Resource Management, The Overseas Chinese Institute of Technology, 100 Chiao-Kwang Road, Taichung 407, Taiwan, R.O.C.

Reprint requests to H.-Y. H.; E-mail: syhsu@ocit.edu.tw

Z. Naturforsch. **62a**, 639–646 (2007); received April 18, 2007

In the present work some transport properties of the binary room temperature molten salt (RTMS) lithium bis(trifluoromethane sulfone)imide (LiTFSI)-acetamide [$\text{LiN}(\text{SO}_2\text{CF}_3)_2\text{-CH}_3\text{CONH}_2$], applied in an Li-ion battery, have been investigated. The phase diagram was determined by differential scanning calorimetry (DSC) and thermogravimetric analysis (TGA). The result reveals that the binary RTMS has an eutectic point at 201 K and the 30 mol% LiTFSI composition. The electric conductivity was measured using a direct current computerized method. The result shows that the conductivities of the melts increase with increasing temperature and acetamide content. The densities of all melts decrease with increasing temperature and acetamide content. The equivalent conductivities were fitted by the Arrhenius equation, where the activation energies were 18.15, 18.52, 20.35, 25.08 kJ/mol for 10, 20, 30, 40 mol% LiTFSI, respectively. Besides the relationships between conductivity, density composition and temperature, of the ion interaction is discussed.

Key words: Room Temperature Molten Salt; Phase Diagram; Conductivity; Density; LiTFSI-Acetamide.

1. Introduction

The lithium-ion battery has widely been applied in camcorders, mobile phones, battery cars and power supply systems owing to its high work voltage, high energy density, stable voltage, long lifetime, wide temperature range and no memory effect, and the high demand of portable electronic devices has increased the importance of compact and reliable lithium secondary batteries. The commercialized lithium-ion batteries use LiPF_6 dissolved in EC-DEC [1]. However, this organic liquid has a high vapour pressure which makes the lithium-ion battery unsafe. Room temperature molten salts (RTMS) possess some unique properties, e. g. wide liquid phase range, high thermal stability, nonflammability, unvolatility and high conductivity [2–5]. Therefore RTMS have attracted much attention as safe electrolytes. RTMS have been widely applied in electrochemical devices such as lithium-ion battery [6–8], super-capacitor [9–11], solar cell [12–16], fuel cell [17, 18] and gas sensor electrode [19–21]. Hussey [22] has noted that industrial exploitation of RTMS looks extremely favourable.

In the present study some transport properties of the binary RTMS lithium bis(trifluoromethane sulfone)-imide (LiTFSI)-acetamide applied in an Li-ion battery were measured. The phase diagram was determined by differential scanning calorimetry (DSC) and thermogravimetric analysis (TGA). The electric conductivities and densities of the binary melts were also measured. The results will contribute to select a better electrolyte for the Li-ion battery.

2. Experimental

LiTFSI (Aldrich, 99.5%) and acetamide (Acros, 99%) were dried at 140 °C and 55 °C, respectively, under vacuum for one week. The molten salts with different molar ratios were prepared by continuous stirring for 24 h under a high purity argon atmosphere in a glove box [Super(1220/750), Mikrouna]. Besides, the water of the melts was measured by Karl-Fischer titration (DL31KF Coulometer, Mettler Toledo).

The phase diagram of the LiTFSI-acetamide melts was obtained by measuring the decomposition temperatures and the melting points. The TGA and DSC analyses were carried out with 5 ~ 10 mg binary melts. The

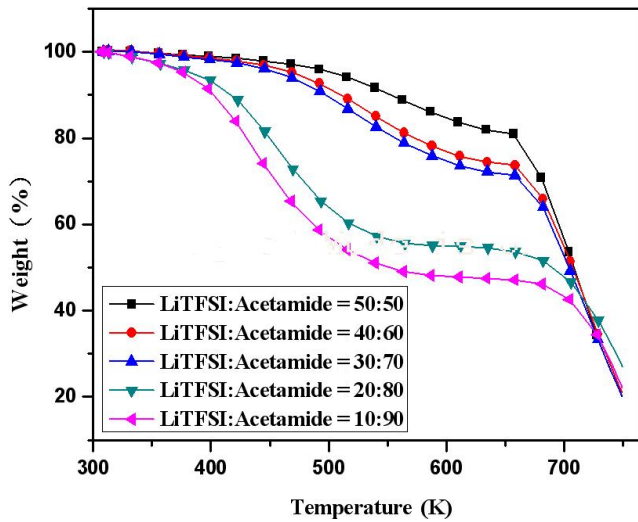


Fig. 1. TGA curves for LiTFSI-acetamide at the molar ratios 10 : 90, 20 : 80, 30 : 70, 40 : 60, 50 : 50.

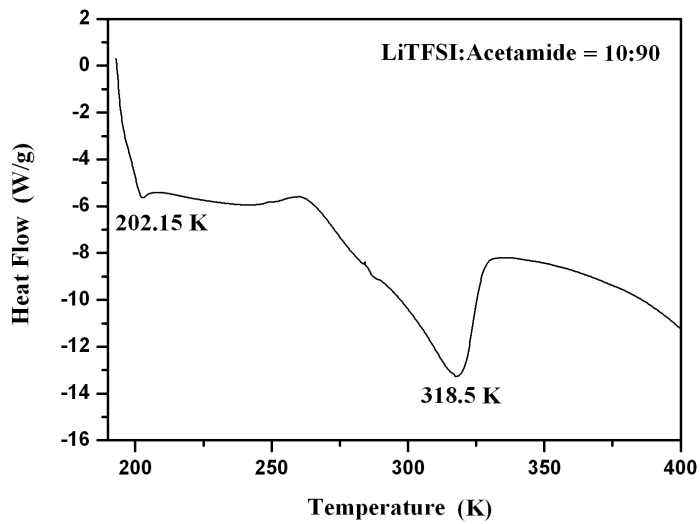


Fig. 2. DSC curve for LiTFSI-acetamide at the molar ratio 10 : 90.

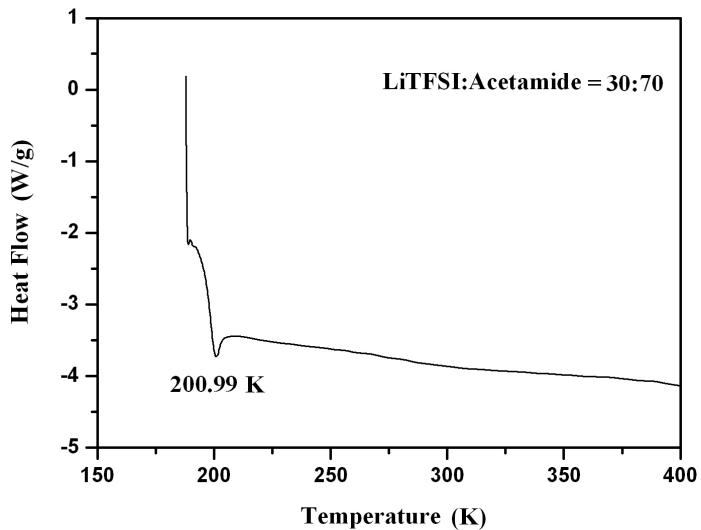


Fig. 3. DSC curve for LiTFSI-acetamide at the molar ratio 30 : 70.

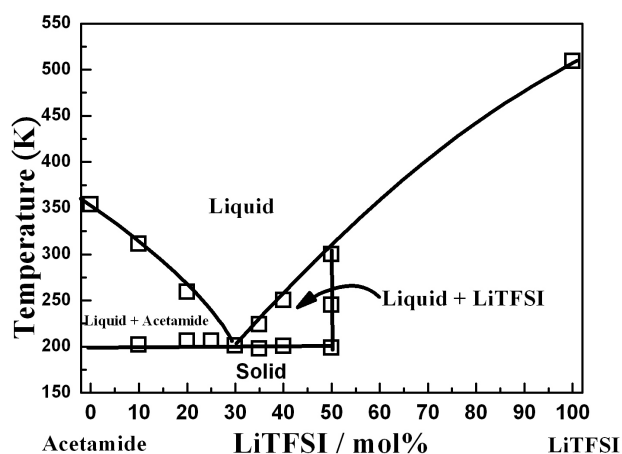


Fig. 4. Liquid-solid phase diagram for the binary $\text{LiN}(\text{SO}_2\text{CF}_3)_2\text{-CH}_3\text{CONH}_2$ molten salt system.

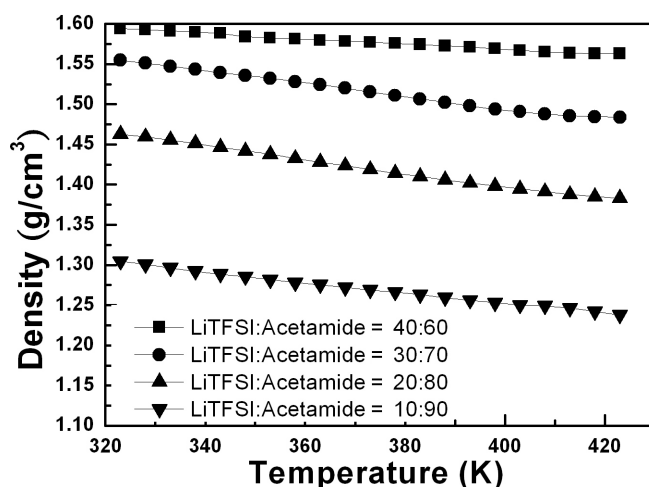


Fig. 5. Density of molten $\text{LiN}(\text{SO}_2\text{CF}_3)_2\text{-CH}_3\text{CONH}_2$ as a function of the temperature.

thermogravimetric analyses of the binary melts were performed on a platinum tray which could be heated from 273 ~ 773 K with a heating rate of 20 K/min. A sealed aluminum disc was used for the DSC analysis. It was, at first, cooled to -60°C by liquid nitrogen. Then the temperature was raised at a rate of 10 K/min. The electric conductivities of the melts were measured using the direct current computerized measurement system designed by Hsu and Yang [23]. The densities of the melts were also determined by using the Archimedes principle, the apparatus being schematically shown in [24].

3. Results and Discussion

The decomposition temperatures were measured by TGA. The results reveal that the decomposition temperatures are around 473 K for different LiTFSI-

acetamide compositions as shown in Figure 1. Figure 2 shows that there are two melting points at 202 K and 319 K for the melt with the molar ratio 10 : 90. Besides, Fig. 3 also shows that there is an apparent melting point at 201 K for the 30 : 70 melt. The DSC analyses were carried out in order to get the melting point for different molar ratio melts. The phase diagram obtained from these data of TGA and DSC analyses is shown in Figure 4. The result reveals that the binary RTMS has an eutectic point at 201 K and the 30 mol% LiTFSI composition. Moreover, the data of the thermal analyses are given in Table 1.

The densities of molten LiTFSI-acetamide as a function of the temperature are shown in Figure 5. The temperature dependence of the density ρ at four compositions is expressed by fitting the equation $\rho = a' + b'/T$, where T is the temperature in K, a' and b' are the parameters given in Table 2. Figure 5 shows that

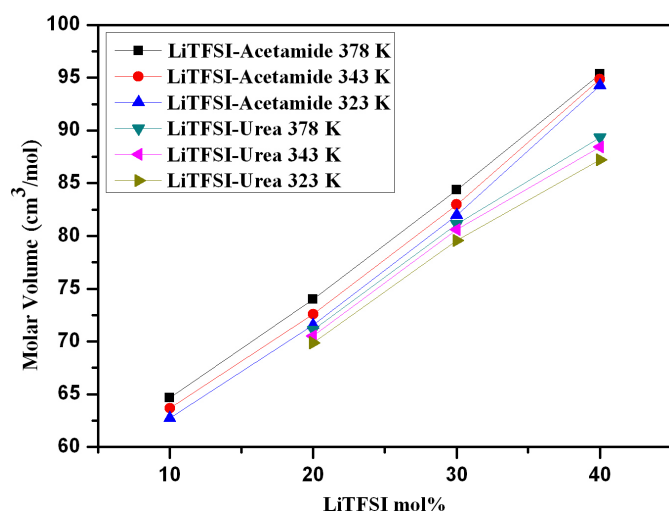


Fig. 6. Isotherms of the molten volume as a function of LiTFSI mole percent in the systems $\text{LiN}(\text{SO}_2\text{CF}_3)_2\text{-CH}_3\text{CONH}_2$ and $\text{LiN}(\text{SO}_2\text{CF}_3)_2\text{-CO}(\text{NH}_2)_2$ at 323, 343, and 378 K.

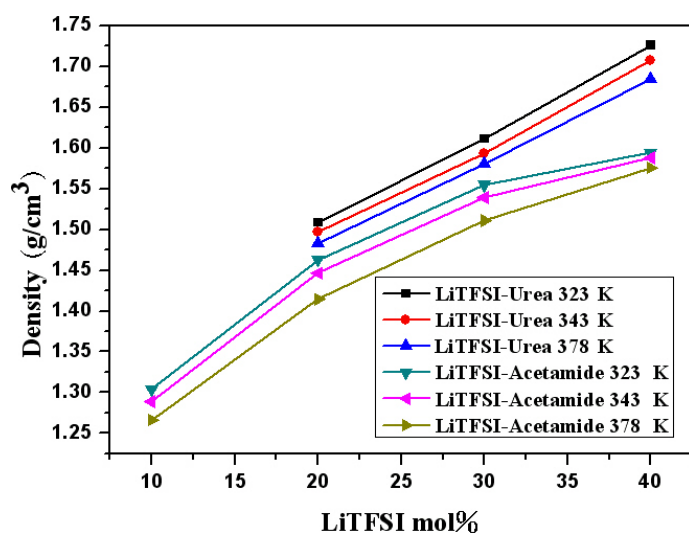


Fig. 7. Isotherms of the density as a function of LiTFSI mole percent in the systems $\text{LiN}(\text{SO}_2\text{CF}_3)_2\text{-CH}_3\text{CONH}_2$ and $\text{LiN}(\text{SO}_2\text{CF}_3)_2\text{-CO}(\text{NH}_2)_2$ at 323, 343, and 378 K.

Table 1. Results of the thermal analysis of LiTFSI-acetamide.

LiTFSI / mol%	Melting point T_m / K	Endothermic enthalpy ΔH / J g^{-1}	Decomposition temperature / K
10	202.15	8.829	423.36
10	318.5	61.01	423.36
20	205.98	3.836	438.43
30	200.99	2.134	463.07
40	200.48	0.9513	524.08
40	250.06	2.581	524.08
50	198.52	2.303	501.55
50	245.35	4.406	501.55

the densities of the four melts decrease with increasing temperature and acetamide content. But the corresponding molar volumes also decrease with increasing the acetamide content, as shown in Figure 6. The re-

Table 2. Density of the binary molten salt LiTFSI-acetamide system, where $\rho = a' + b'T$.

LiTFSI / mol%	a' / g cm^{-3}	b' / $10^{-4} \text{ g cm}^{-3} \text{ K}$	R-Square	T / K
10	1.509	-6.44	0.9961	323–423
20	1.732	-8.373	0.9960	323–423
30	1.802	-7.689	0.9925	323–423
40	1.699	-3.264	0.9922	323–423

sult is not similar to the reported studies for $\text{ZnCl}_2\text{-DMSO}_2$ [24] and $\text{FeCl}_3\text{-DMSO}_2$ [25]. The reason is that the molecular mass of LiTFSI (287 g/mol) is larger than that of acetamide (59.07 g/mol), resulting in a substantial decrease of the mean molecular mass if the molar ratio of acetamide increases. In order to better study this phenomenon, acetamide was replaced by urea. The

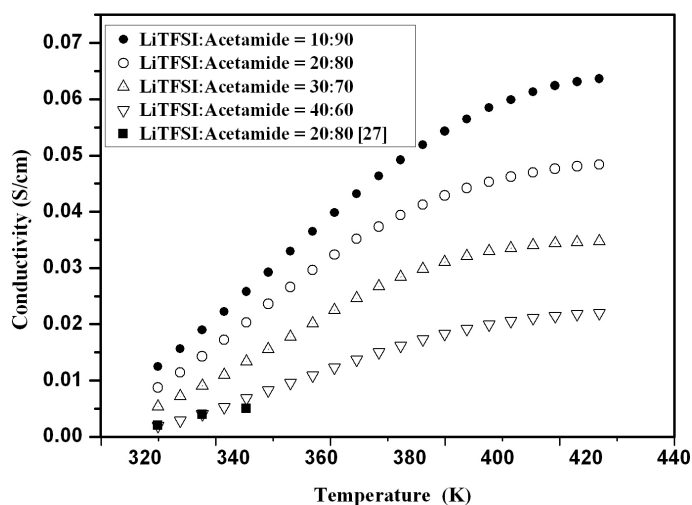


Fig. 8. Electrical conductivity of molten LiN-(SO₂CF₃)₂-CH₃CONH₂ as a function of the temperature.

result is also shown in Figure 6. Moreover, the densities of acetamide and urea as a function of LiTFSI mole percent are also shown in Figure 7. The result indicates that the densities of the LiTFSI-urea system are higher than those of the LiTFSI-acetamide system.

With regard to the effect of the two organic compounds to the formation of RTMS, it can be assumed that the two organic compounds work as complex agents for both cations and anions due to their polar groups. Hu *et al.* [26] have studied the RTMS of LiTFSI-urea and LiTFSI-acetamide. They indicated that the polar groups (C=O group and NH₂ group) of urea and acetamide are capable of coordinating with cations and anions, respectively, leading to weakening and even breaking the bonding between the Li⁺ cations and TFSI⁻ anions. The interactions lead to the breaking of the hydrogen bonds between organic molecules and the weakening of the Coulombic interaction between the anions and cations of LiTFSI. However, owing to the urea molecule having three polar groups (C=O group and two NH₂ groups), the urea molecule in the binary melt will have a stronger interaction than the acetamide molecule. Therefore, the LiTFSI-acetamide melt has a bigger molar volume, as shown in Figure 6.

The relationship between the conductivity and temperature of the binary RTMS electrolyte with several compositions is shown in Figure 8. The result shows that the conductivities of the binary RTMS increase with increasing temperature and acetamide content. The movement of the ions and the molar volume of the melt increase with temperature, resulting in an increasing ionic mobility. Gruthner [27] has reported that the

conductivity of pure molten acetamide has the characteristic of self-ionization or auto-protolysis, which can also be found in water.

The reaction is



The ionization causes an amphiprotic acid-base character of acetamide. In this study, a decrease of the conductivity with increasing the content of salt (LiTFSI) has been confirmed. However, the increase of the acetamide content increases not only the free space but also the mobility of the disassociated species. The result is consistent with the observation reported by Hu *et al.* [26].

Figure 9 shows the conductivities of the LiTFSI-acetamide and LiTFSI-urea RTMS as a function of the LiTFSI mole fraction at several temperatures. The result reveals that the LiTFSI-acetamide RTMS has a higher conductivity. The result may be explained in terms of the interactions among the solute and the solvent. Since the acetamide molecule has two polar groups (C=O and NH₂), the interaction of acetamide is weaker than that of urea (three polar groups). As a result, the LiTFSI-acetamide RTMS has a larger molar volume and mobility. Therefore, a result as shown in Fig. 9 is obtained.

The interactions and bonding of LiTFSI and acetamide in the binary RTMS are shown in Figure 10. It is clear that, since the oxygen atom has a larger electronegativity (EN = 3.5), the Li⁺ ion has a tendency to coordinate with the O(22) atom in the C=O group of acetamide. Hu *et al.* [28] have indicated that, since

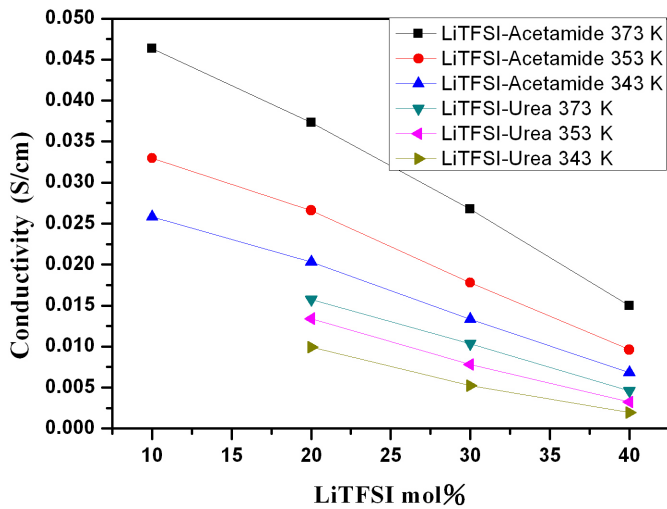


Fig. 9. Isotherms of the electrical conductivity as a function of LiTFSI mole percent in the systems $\text{LiN}(\text{SO}_2\text{CF}_3)_2\text{-CH}_3\text{CONH}_2$ and $\text{LiN}(\text{SO}_2\text{CF}_3)_2\text{-CO}(\text{NH}_2)_2$ at 343, 353, and 373 K.

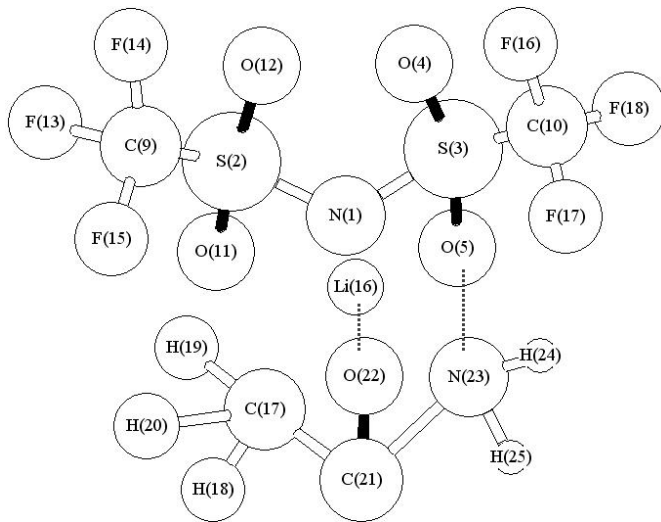


Fig. 10. The most stable structure of the LiTFSI-acetamide complex.

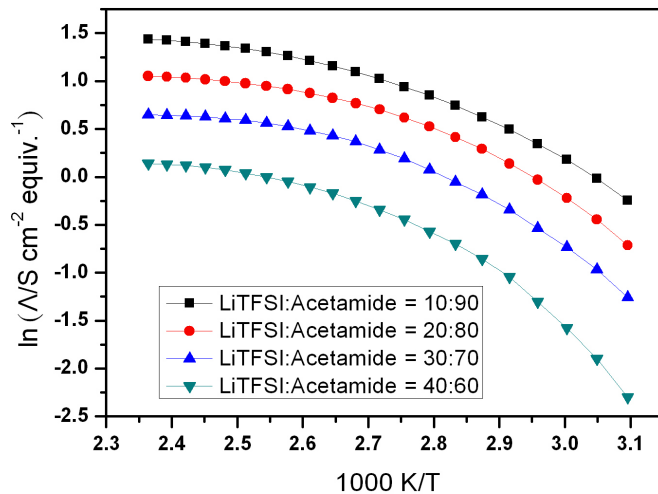


Fig. 11. Arrhenius plots of the equivalent conductivity of molten $\text{LiN}(\text{SO}_2\text{CF}_3)_2\text{-CH}_3\text{CONH}_2$.

Table 3. Activation energy from Arrhenius fits of the electrical conductivity and equivalent conductivity of the binary molten salt, LiTFSI-acetamide system, where $\kappa = \kappa_0 \exp(-E_\kappa/RT)$ and $\Lambda = \Lambda_0 \exp(-E_\Lambda/RT)$.

LiTFSI / mol%	$E_\kappa / \text{kJ mol}^{-1}$	$E_\Lambda / \text{kJ mol}^{-1}$
10	22.12	18.15
20	23.53	18.52
	3.97*	
30	26.19	20.35
40	32.53	25.08

* LiTFSI : acetamide = 20 : 80 from [27].

there is a large amount of O atoms in acetamide interacting with Li^+ ions, a stronger cation-solvent interaction occurs when the acetamide concentration is high. Moreover, the SO_2 group of TFSI⁻ anions interacts with the NH_2 group of acetamide via hydrogen bonding. However, these interactions among solute and solvent will affect significantly the conductivity of binary RTMS. Besides, Hu *et al.* have also indicated that the ionic association increases with increasing salt concentration, resulting in a considerable amount of contact ion pairs. Therefore, the ionic conductivity decreases. It can be concluded that the ionic conductivity strongly depends on the ionic association in the complex system.

The equivalent conductivities are fitted by the Arrhenius equation $\Lambda = \Lambda_0 \exp(-E_\Lambda/RT)$ for several LiTFSI-acetamide RTMS as shown in Figure 11. The parameters of the activation energies for the isotherms of the electric conductivity and equivalent conductivity are given in Table 3. Generally, a molten salt with low

lattice energy tends to show a high ionic migration, because a low dissociation energy increases the number of free ions. Thus, the 10 mol% LiTFSI RTMS has the lowest equivalent conductivity and electric conductivity activation energies among the investigated compositions. Both activation energies are closely linked, and E_κ is always greater than E_Λ in the LiTFSI-acetamide system. Similarity between E_κ and E_Λ is indicative of ionic packing or complex formation in the melt.

4. Conclusion

The phase diagram of LiTFSI-acetamide RTMS is obtained. The result reveals that the binary RTMS has an eutectic point at 201 K and the 30 mol% LiTFSI composition. The densities of all melts decrease with increasing temperature and acetamide content. Furthermore, the corresponding molar volumes also decrease with increasing acetamide content. The reason has been given. The electric conductivity is measured using a direct current computerized method. The results show that the conductivities of the melts increase with increasing temperature and acetamide content. The characteristic changes of the binary RTMS have been explained by the ion interaction among the melt electrolytes.

Acknowledgement

This work is supported by the National Science Council, Taiwan, Republic of China, under Contract NSC 94-2214-E-224-005 / NSC 95-2221-E-224-064.

- [1] E. Mashiko, M. Yokokawa, and T. Nagura, *Proceedings of the 2nd Battery Symposium*, Tokyo, Japan, 1B2, 31 (1991).
- [2] R. J. Gale and D. G. Lovering, *Molten Salt Techniques*, Vol. 4, Plenum Press, New York 1983, pp. 1–4.
- [3] J. Sun, M. Forsyth, and D. R. MacFarlane, *J. Phys. Chem. B* **102**, 8858 (1998).
- [4] D. R. MacFarlane, P. Meakin, J. Sun, N. Amini, and M. Forsyth, *J. Phys. Chem. B* **103**, 4164 (1999).
- [5] B. Vestergaard, N. J. Bjerum, I. Petrushina, H. A. Hjuler, R. W. Gerg, and M. Begtrup, *J. Electrochem. Soc.* **140**, 3108 (1993).
- [6] D. R. MacFarlane, P. Sun, N. Amini, and M. Forsyth, *J. Phys. Chem. B* **103**, 4164 (1999).
- [7] H. Matsumoto, M. Yanagida, K. Tanimoto, M. Nomura, Y. Kitagawa, and Y. Miyazaki, *Chem. Lett.* **29**, 922 (2000).
- [8] H. Matsumoto, H. Kageyama, and Y. Miyazaki, *Chem. Commun.*, 1726 (2002).
- [9] C. Nanjundiah, S. F. McDenitt, and V. R. Koch, *J. Electrochem. Soc.* **144**, 3392 (1997).
- [10] A. B. McEwen, S. F. McRevitt, and V. R. Koch, *J. Electrochem. Soc.* **144**, L84 (1997).
- [11] M. Ue, M. Takeda, T. Takahashi, and M. Takehara, *Electrochem. Solid State Lett.* **5**, A119 (2002).
- [12] B. O'Regan and M. Grätzel, *Nature* **353**, 727 (1991).
- [13] A. Hagfeldt and M. Grätzel, *Chem. Rev.* **95**, 49 (1995).
- [14] N. Papageorgiou, Y. Athansson, M. Armand, P. Bonhôte, H. Pettersson, A. Azam, and M. Grätzel, *J. Electrochem. Soc.* **143**, 3009 (1996).
- [15] H. Matsumoto, *Electrochemistry* **70**, 190 (2002).
- [16] H. Mateumtot, T. Mateuda, T. Tsuda, R. Hagiwara, Y. Ito, and Y. Miyazaki, *Chem. Lett.* **30**, 26 (2001).
- [17] B. C. H. Steele and A. Heinzl, *Nature* **414**, 345 (2001).
- [18] K. D. Kreuer, *ChemPhysChem* **3**, 771 (2002).
- [19] W. Kakashima, M. Kaneko, K. Kaneto, and A. G. MacDiarmid, *Synth. Met.* **71**, 2265 (1995).

- [20] E. Smela, O. Inganas, and I. Lundstrom, *Science* **268**, 1735 (1995).
- [21] W. Lu, A. G. Fadeev, B. Qi, E. Smela, B. R. Mattes, J. Ding, G. M. Spinks, J. Mazurkiewicz, D. Zhou, G. G. Wallace, D. R. MacFarlane, S. A. Forsyth, M. Forsyth, *Science* **297**, 983 (2002).
- [22] C. L. Hussey, *Electrochemistry* **67**, 527 (1999).
- [23] H. Y. Hsu and C. C. Yang, *Z. Naturforsch.* **56a**, 570 (2001).
- [24] M. F. Shu, H. Y. Hsu, and C. C. Yang, *Z. Naturforsch.* **58a**, 451 (2003).
- [25] C. C. Yang, M. F. Shu, and P. Y. Cheng, *Z. Naturforsch.* **60a**, 848 (2005).
- [26] Y. Hu, H. Li, X. Huang, and L. Chen, *Electrochem. Commun.* **6**, 28 (2004).
- [27] B. Gruthner, *Z. Anorg. Allg. Chem.* **270**, 223 (1952).
- [28] Y. Hu, Z. Wang, H. Li, X. Huang, and L. Chen, *J. Electrochem. Soc.* **151**, A1424 (2004).